Title

Realistic magnetic thermodynamics by local quantization of a semiclassical Heisenberg model

Journal

npj Computational Materials, 8(1)

ISSN

2057-3960

Authors

Walsh, Flynn

Asta, Mark

Wang, Lin-Wang

Publication Date

2022

DOI

10.1038/s41524-022-00875-8

npj computational materials

www.nature.com/npjcompumats

ARTICLE OPEN

Check for updates

Realistic magnetic thermodynamics by local quantization of a semiclassical Heisenberg model

Flynn Walsh[1,2], Mark Asta[1,3]✉ and Lin-Wang Wang[1,4]✉

Classical Monte Carlo simulation of the Heisenberg model poorly describes many thermodynamic phenomena due to its neglect of the quantum nature of spins. Alternatively, we discuss how to semiclassically approach the quantum problem and demonstrate a simple method for introducing a locally approximate form of spin quantization. While the procedure underestimates magnetic short-range order, our results suggest a simple correction for recovering realistic spin–spin correlations above the critical temperature. Moreover, ensemble fluctuations are found to provide reasonably accurate thermodynamics, largely reproducing quantum mechanically calculated heat capacities and experimental magnetometry for ferromagnetic Fe and antiferromagnetic $RbMnF_3$. Extensions of the method are proposed to address remaining inaccuracies.

npj Computational Materials (2022)8:186 ; https://doi.org/10.1038/s41524-022-00875-8

INTRODUCTION

The Heisenberg model has been widely studied as both a classical and quantum description of crystal magnetism. In either interpretation, the Hamiltonian can be expressed as:

$$H = -\sum_{i,j} J_{ij}\,\mathbf{S}_i \cdot \mathbf{S}_j \tag{1}$$

where i and j sum over lattices sites and J_{ij} is an interaction energy determined by the relative positions of i and j. Classically, $\mathbf{S}_i$ is a dimensionless spin vector proportional to local magnetic moment. While atomic magnetism has fundamentally quantum origins, the classical model largely accounts for the energies of static spin configurations, reproducing experimental magnon spectra and capturing magnetic contributions to the energies of electronic structure calculations[1,2]. It does not, however, accurately describe thermodynamic properties below the magnetic disordering temperature[3,4] and, while alternatives have been proposed[3–10], the efficient simulation of finite temperature magnetism remains an outstanding problem in computational materials science.

The limited success of the classical Heisenberg model can be understood by regarding classical moments as the quantum expectation values of spin operators, as is detailed in the following section. With this perspective, we consider Monte Carlo (MC) simulation of the Heisenberg model, a popular approach to calculating thermodynamic properties by probabilistically sampling the spin-configuration space. The deficiency of classical MC (CMC) methods is addressed and a more accurate, but similarly general, semiclassical MC (SMC) sampling technique is proposed, demonstrated, and discussed.

RESULTS

Background and motivation

In the more physical quantum Heisenberg model, $\mathbf{S}_i$ operates on spinor $|\chi_i\rangle$ to measure the spin of lattice site i. N spins of quantum number s form a $(2s+1)^N$-dimensional Hilbert space. A canonical system in thermal equilibrium is described by density operator $\rho = e^{-\beta H}/Z$, where partition function $Z = \mathrm{tr}(e^{-\beta H})$ and β is the reciprocal product of Boltzmann's constant and temperature. Thermodynamic quantities corresponding to ensemble averages, such as energy or magnetization, are determined from ρ as $\overline{O} = \langle O\rangle = \mathrm{tr}\,(\rho O)$, where $\overline{O}$ denotes the ensemble average and $\langle O\rangle$ indicates a quantum expectation value.

Density operators are typically expanded as sums over energy eigenstate projectors, although the eigensystem of Eq. (1) is not generally solvable. Instead, states may be sampled through quantum MC (QMC) techniques[11], although current methods appear numerically unstable for Hamiltonians containing competing interactions[12], such as geometric frustration[13] or even values of J_{ij} with opposing signs[14], as is often the case in real materials. Compared to CMC, QMC is also far more conceptually and computationally complex, with simulation time scaling nonlinearly with system size[15].

Fortunately, magnets that are not significantly entangled may not require a full quantum treatment. Above some temperature, all equilibrium systems become unentangled, or separable[16], meaning that ρ may be expressed as a sum over product states $|\psi_p\rangle = |\chi_1\rangle \otimes |\chi_2\rangle \cdots \otimes |\chi_N\rangle$. Entanglement phenomena have been primarily identified in one or two-dimensional systems at low temperatures[17,18], so we assume that separability is at least a very a good approximation for conventional three-dimensional magnets above a few degrees Kelvin.

Product states are attractive because their expectation values distribute across components of the tensor product[19], enabling effectively classical evaluation of the Heisenberg Hamiltonian. For product state $|\psi_p\rangle$, energy E_p can be determined as:

$$\langle H\rangle_p = -\sum_{i,j} J_{ij}\,\langle \mathbf{S}_i \cdot \mathbf{S}_j\rangle_p = -\sum_{i,j} J_{ij}\,\langle \mathbf{S}_i\rangle_p \cdot \langle \mathbf{S}_j\rangle_p, \tag{2}$$

where $\langle O\rangle_p$ denotes $\langle\psi_p|O|\psi_p\rangle$. Equation (2) explains the success of the classical Heisenberg model in evaluating the energies of given magnetic structures, if classical $\mathbf{S}_i$ is understood as quantum $\langle \mathbf{S}_i\rangle_p$.

When $\langle \mathbf{S}_i\rangle_p$ is not prescribed, however—as is typically the case for thermodynamic ensembles—classical methods are far less accurate

[1]Materials Sciences Division, Lawrence Berkeley National Laboratory, Berkeley, CA 94720, USA. [2]Graduate Group in Applied Science and Technology, University of California, Berkeley, CA 94720, USA. [3]Department of Materials Science and Engineering, University of California, Berkeley, CA 94720, USA. [4]Present address: Institute of Semiconductors, Chinese Academy of Sciences, 100083 Beijing, China. ✉email: mdasta@berkeley.edu; lwwang@semi.ac.cn

as determining which values of $\langle \mathbf{S}_i \rangle_p$ to consider requires significant approximation. Most notably, conventional CMC simulations sample spin states continuously, which is only justified in the limit of an infinite spin quantum number[20,21]. Taking this limit provides the standard derivation of the classical Heisenberg model and leads to a scaling relation between the quantum (J_{ij}) and classical (J_{ij}^{∞}) interaction energies for spin quantum number s:

$$s(s+1)J_{ij} = s^2 J_{ij}^{\infty}. \tag{3}$$

Perhaps unsurprisingly, the assumption of infinite s causes unphysical thermodynamic behavior in not only CMC, but also classical spin dynamics simulations[22].

However, if $\langle \mathbf{S}_i \rangle_p$ were known for all the components of a separable representation, its thermodynamic properties could be calculated with quantum accuracy and classical convenience. For a separable ensemble that can be represented in terms of product states p, the average of observable O may be expressed as a classical sum, i.e.:

$$\overline{O} = \frac{1}{Z}\sum_p \mathrm{e}^{-\beta E_p} \langle O \rangle_p, \tag{4}$$

as detailed in Supplementary Note 1. For the determination of $\overline{E}$, Eq. (2) can be substituted into Eq. (4) such that the ensemble average is expressed in terms of $\langle \mathbf{S}_i \rangle_p$, with a similar procedure possible for other thermodynamic properties. Of course, identifying specific $|\psi_p\rangle$ or $\langle \mathbf{S}_i \rangle_p$ is no easier than determining eigenstates, but it may be feasible to approximate the density of product states more accurately than classical methods. Indeed, representatively sampling states in a high-dimensional configuration space is the fundamental purpose of MC simulations.

Previous efforts to improve the accuracy of classical simulations can be understood from this perspective. For example, spin-wave excitations can be quantized using Planck statistics, which reasonably describe magnetization behavior[1], although local updating methods are generally far more efficient for atomistic simulations. Ref. [8] approximates a density of states explicitly calculated using first-principles methods by introducing and adjusting an effective simulation temperature. This approach, which can be applied in continuous time spin dynamics as well as MC simulations[9], works well at low temperatures, but requires parameterization and underestimates[8] (or overestimates[9]) magnetization at intermediate temperatures. Somewhat similarly, ref. [7] describes a method for empirically determining effective temperatures, while ref. [10] reproduces a Planck distribution through careful control of a spin dynamics thermostat. It is also worth noting that the methods of refs. [3,7–9] directly depend on the Curie temperature (T_C), above which CMC is performed.

Semiclassical sampling by local quantization

Alternatively, we propose a more direct approach for estimating the separable density of states based on a locally quantum approximation of state evolution. In the simplest form of CMC, a new state is trialed by mutating the (expected) spin of randomly selected site k, while the spins of all other sites $i \neq k$ are fixed. Trial $\langle \mathbf{S}_k \rangle$ is traditionally chosen with uniform probability for all directions, as is classically allowed. However, it is possible to introduce an approximate quantization by treating this ultimately fictitious permutation as a quantum problem.

In this approach, Eq. (1) can be reframed as a single-spin quantum Hamiltonian for site k:

$$H_k = E_{i\neq k} - \mathbf{S}_k \cdot 2\sum_j J_{kj} \langle \mathbf{S}_j \rangle, \tag{5}$$

where $\langle \mathbf{S}_j \rangle$ is the fixed spin of neighboring site j. (The factor of two originates from the double summation in Eq. (1)). As $E_{i\neq k}$ is constant, Eq. (5) has the elementary solutions of a spin in the magnetic field $\mathbf{B}_k = 2\sum_j J_{kj} \langle \mathbf{S}_j \rangle$. Specifically, $\mathbf{S}_k$ is quantized along

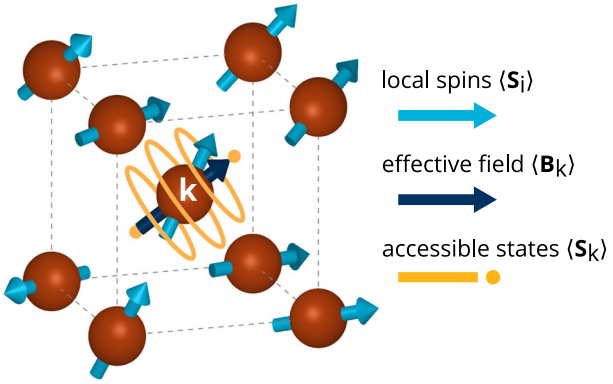

Fig. 1 MC trial states allowed by local quantization. An illustration of the semiclassical spin sampling procedure on a bcc lattice with $s = 2$. Site k is randomly selected and the effective local field $\mathbf{B}_k$ is determined from the fixed spins of neighboring sites $\langle \mathbf{S}_j \rangle$ and the interaction energies J_{kj}. A new trial value of $\langle \mathbf{S}_k \rangle$ is randomly selected from the illustrated quantizations along $\mathbf{B}_k$.

$\mathbf{B}_k$ with quantum number $m_s = -s, -s+1, \ldots, s$; its orthogonal components are inherently uncertain, but their expectation values precess around $\mathbf{B}_k$ in time.

The solutions of Eq. (5) can be statistically sampled according to the following SMC procedure, which is illustrated in Fig. 1. For each MC step, site k is randomly selected and $\mathbf{B}_k$ is computed. A trial quantization along $\mathbf{B}_k$ (corresponding to some m_s) is chosen at random, defining the component of $\langle \mathbf{S}_k \rangle$ along $\mathbf{B}_k$; any remaining perpendicular component is then randomly chosen to account for continuous precession. The accessible trial states $\langle \mathbf{S}_k \rangle$ for a hypothetical scenario are drawn as rings around $\mathbf{B}_k$ in Fig. 1. The trial energy is computed and acceptance or rejection is determined according to the standard Metropolis criteria, after which a new k is chosen for the next step. In practice, SMC requires only marginally more effort than CMC, with spin quantum number s being the only additional parameter.

While the impact of multiple-spin interactions on quantization has been neglected, these solutions should still estimate the true distribution of product states better than purely classical methods, although the extent of the improvement is not immediately clear as separable solutions of large ensembles are generally intractable. In practice, the results are notably more accurate—indeed, the remainder of this paper demonstrates how locally quantized SMC reasonably describes thermodynamic properties across a wide temperature range, albeit with several caveats.

Magnetization of Fe

The zero-field spontaneous magnetization of body-centered cubic (bcc) Fe provides a classic benchmark for finite temperature magnetic predictions. Figure 2 shows measurements from ref. [23] alongside notably differing CMC calculations (see Methods for details). The experimental ground state moment of 2.2 μ_B/atom implies a quantum number of $s = 1.1$, neglecting orbital contributions that are suppressed under the system's cubic symmetry. As a transition metal, the itinerant magnetism of Fe is less than perfectly described by a collection of atomic spinors, but the standard Heisenberg model appears to provide a passable approximation[24]. Previous studies have modeled Fe by interpolating results for $s = 1$ and $s = 3/2$[3], but for the purpose of demonstration, Fig. 2 shows distinct SMC magnetization curves for $s = 1$, 3/2, and 2.

All the quantized calculations greatly improve upon CMC, although no single value of s exactly replicates experiment. Using $s = 1$, as is closest to the experimentally implied value, provides the best results near T_C, but not at lower temperatures, where

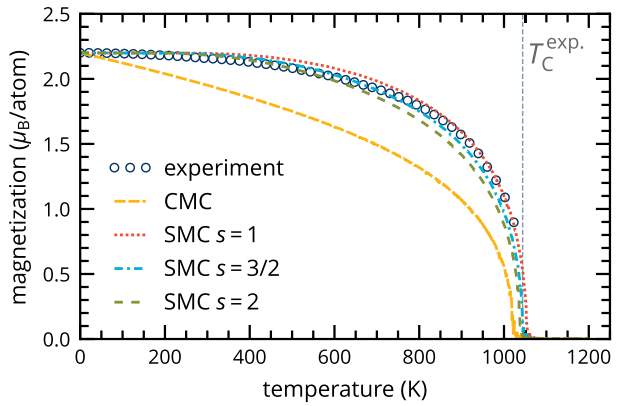

Fig. 2 Spontaneous magnetization of iron. Spontaneous magnetization of elemental (bcc) Fe as a function of temperature, determined using CMC and SMC sampling for several spin quantum numbers s and experiment[23].

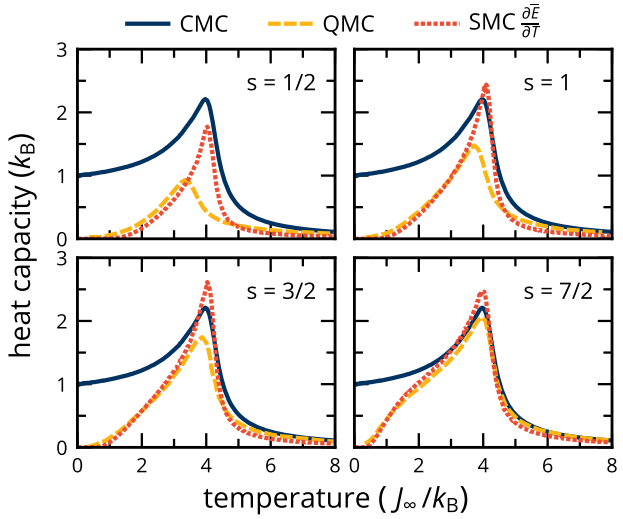

Fig. 3 Heat capacity of a model ferromagnet for several spin quantum numbers. Heat capacity of a bcc nearest neighbor ferromagnets for varying spin quantum number s, calculated via CMC, QMC (adapted from ref. [3]), and SMC according to Eq. (6) Nearest neighbor interaction energies are determined from classical J_∞ by Eq. (3).

$s = 3/2$ appears slightly more accurate. The next highest value of $s = 2$ is generally further from experiment, expectedly approaching the classical limit of infinite s—the gradual convergence of CMC and SMC is further shown in Supplementary Fig. 2. Critical magnetization behavior is also examined in Supplementary Fig. 3. Some remaining inaccuracies are discussed later, but the overall dramatic improvement clearly shows the potential of semiclassical local quantization.

Heat capacity and magnetic short-range order

While demonstrative, direct comparison of computational predictions to experiments is complicated by the many levels of approximation inherent in the theory. Fortunately, ref. [3] provides effectively exact QMC heat capacities for a small bcc ferromagnet with nearest neighbor Heisenberg interactions, which are shown in Fig. 3 for four spin quantum numbers in addition to infinite spin CMC (see Methods for details). Heat

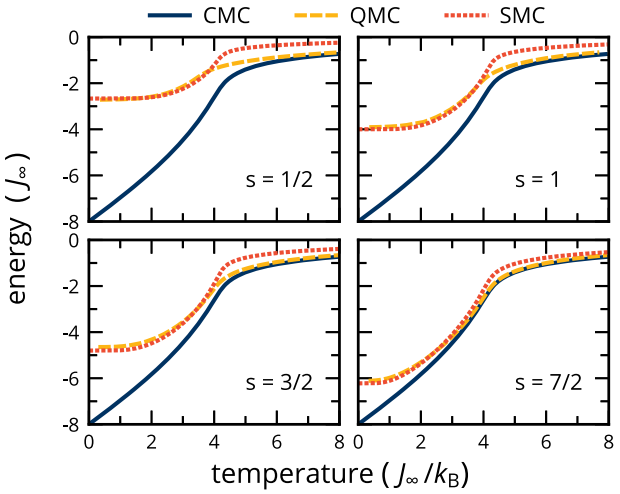

Fig. 4 Energy of a model ferromagnet for several spin quantum numbers. Analogous to Fig. 3, the energies of a bcc ferromagnet with varying quantum number s according to CMC, QMC, and SMC. While SMC appears to reproduce the QMC of ref. [3] below the disordering point, higher temperature energies are overestimated due to missing short-range order.

capacity is defined as:

$$C = \frac{\partial \bar{E}}{\partial T}, \tag{6}$$

from which many other thermodynamic properties can be derived. Figure 3 shows that direct calculation of SMC heat capacity according to Eq. (6) largely reproduces QMC at lower temperatures, but results in significant errors around T_C, with altogether less improvement over CMC than seen in Fig. 2.

An explanation for excessive heat capacity in the critical region follows from Eq. (6); overestimation of heat capacity implies that simulation energies increase too rapidly with respect to temperature, which is explicitly shown in Fig. 4. Below T_C, semiclassical energies closely track QMC values, but magnetic disordering imparts a rapid increase in energy, resulting in an overestimation of energy that only gradually disappears at higher temperatures. Excess energies indicate that these simulations are less ordered than their QMC counterparts—since the error only becomes significant as long-range order disappears, it is apparent that locally quantized SMC systematically underestimates magnetic short-range order (MSRO).

In contrast, Fig. 4 shows how CMC energies are correct in the high-temperature limit despite significant error below T_C. Nonetheless, CMC and SMC predict very similar degrees of order above T_C, as demonstrated in Fig. 5 for nearest neighbor spins in bcc Fe. These two observations imply that accurate CMC energies (and related properties, such as heat capacity) above T_C originate from the $\frac{s+1}{s}$ energetic scaling that was introduced in Eq. (3). Indeed, CMC has long been believed to underestimate MSRO on the basis of both experiment[25,26] and theory[27–30]. As a reference, Fig. 5 includes the significantly more ordered predictions[30] of dynamic spin-fluctuation theory[31], an advanced linear-response technique that does not explicitly consider local moments.

The observation that scaling CMC interaction parameters, as is required to preserve the Curie temperature, leads to accurate energies above T_C implies that a similar correction factor could recover realistic MSRO. This simple idea is tested in Fig. 5, which includes a version of the CMC spin–spin correlations multiplied post hoc by $\frac{s+1}{s}$ (for $s = 1.1$) that favorably compares to the theory of ref. [30]. The remaining discrepancy may be attributable to the neglect of longitudinal spin fluctuations, which, although relatively

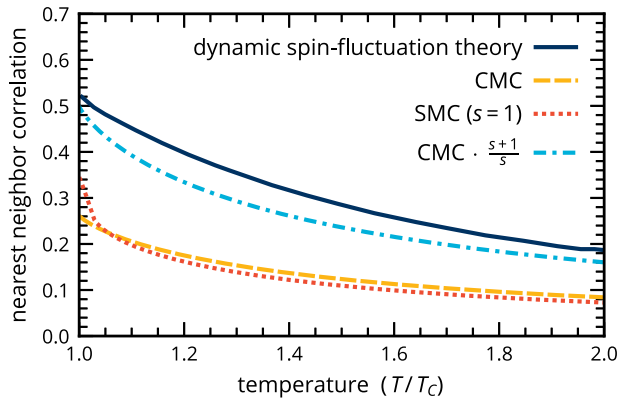

Fig. 5 Magnetic short-range order in iron. Predictions of MSRO in bcc Fe by several theories, represented by the normalized nearest neighbor spin–spin correlation: $\mathbf{S}_i \cdot \mathbf{S}_j / (\overline{S_i} \overline{S_j})$ for nearest neighbors i and j. Very similar CMC and SMC results are compared to dynamic spin-fluctuation theory[30], which predicts significantly larger MSRO due to quantization effects. The discrepancy can be mostly eliminated using the $\frac{s+1}{s}$ correction factor deduced from comparison of QMC and CMC.

small in Fe, can significantly affect MSRO[24], as well as the specific parameterization of the Hamiltonian.

The proposed scaling factor offers a path for correcting SMC, either post hoc or possibly through scaling interaction parameters J_{ij} as in CMC. With an optimized interpolation scheme smoothly introducing the scaling factor across the critical region, SMC could conceivably replicate QMC across across all temperatures in a manner reminiscent of previously employed techniques[3,7]. However, this approach would compromise much of the convenience of SMC and a somewhat more straightforward method for recovering accurate heat capacities is explored in the following section.

Improved accuracy from fluctuations

Heat capacity may alternatively (and more conventionally) be calculated according to the fluctuation-dissipation theorem, i.e.:

$$C = \frac{\overline{E^2} - \overline{E}^2}{k_B T^2}, \tag{7}$$

which must equal Eq. (6) for a statistically valid ensemble. However, SMC heat capacities determined in this manner, plotted in Fig. 6, notably differ from those previously calculated in Fig. 3—in fact, the values obtained from the fluctuation-dissipation theorem are significantly closer to the QMC of ref. [3].

The disagreement between the heat capacities calculated from Eqs. (6) and (7) can be attributed to a violation of balance by the SMC sampling procedure. Local quantization clearly does not satisfy *detailed* balance, as the local field at any site is frequently changed as neighboring spins are reoriented. If a spin is re-quantized along an updated local field, it is likely impossible to directly return to the prior state along the former quantization axis, which is a fundamental requirement for detailed balance. It is less immediately obvious that this procedure violates the statistically necessary condition of balance[32], but the difference between the two methods of calculating heat capacity, which are formally equivalent for a properly sampled ensemble, suggest an absence of balance. In contrast, if all spins are quantized along a fixed axis, then (detailed) balance is recovered and both methods of calculating heat capacity predict consistent values, which are similar to those of Fig. 3 (this is explicitly shown in Supplementary Fig. 1). For local quantization, issues of balance could be circumvented by performing non-Markovian MC such as

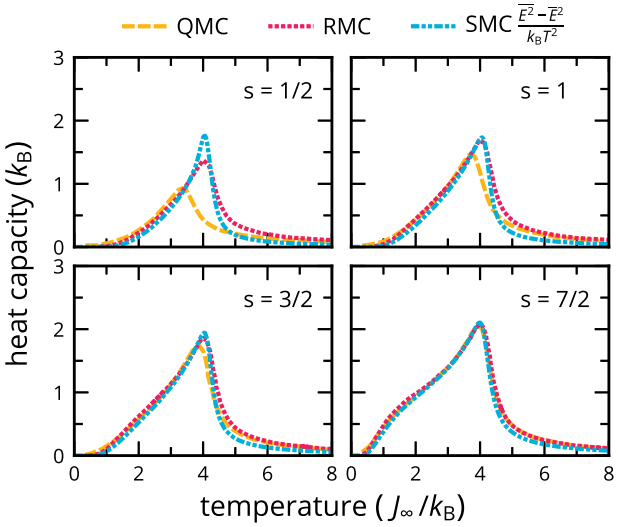

Fig. 6 Improved and benchmarked heat capacities of the model ferromagnet. The QMC heat capacities from Fig. 3 (and ultimately ref. [3]) compared to SMC calculations using Eq. (7), which are significantly more accurate than those shown in Fig. 3. The "rescaled" MC (RMC) results from ref. [3], which provide a similar degree of accuracy, are also shown.

Wang-Landau sampling[33], which determines $\overline{E^2}$ from a sampled distribution of E such that Eq. (7) reproduces Eq. (6).

However, the degree of accuracy shown in Fig. 6 suggests that the fluctuation-based calculations are capturing more realistic physics. Despite excessive average energies due to the underestimation of MSRO, the SMC calculations appear to sample realistic energetic fluctuations. As shown in Fig. 3, the heat capacities of Eq. (6) are about as accurate as the best existing methods for (non-quantum) magnetic thermodynamics, exemplified by the "rescaled" MC of ref. [3], which applies an empirical correction factor to CMC based on lattice-specific QMC for a model Hamiltonian. The fluctuation-based approach thus seems very promising for practical calculations, although it would benefit from a more rigorous explanation for the demonstrated accuracy.

Antiferromagnetic susceptibility of $RbMnF_3$

While only ferromagnets have been considered up to this point, SMC sampling works similarly well for antiferromagnets, of which $RbMnF_3$ is one of the simplest examples. In this compound, Mn ions form a simple cubic sublattice with $s = 5/2$ and effectively nearest neighbor exchange interactions[34]. Figure 2 shows the zero-field parallel susceptibility ($\chi^{\parallel}$) of $RbMnF_3$, both from experiment[35] and calculated with CMC and SMC via the fluctuation-dissipation theorem:

$$\chi^{\parallel} = \frac{\overline{\mathbf{M}^2} - \overline{\mathbf{M}}^2}{k_B T}. \tag{8}$$

Both axes have been scaled relative to T_N values to ease comparison with experiment. SMC is expectedly far more accurate than CMC below the disordering point, although $\chi^{\parallel}$ is somewhat underestimated at very low temperatures. Classical $\chi^{\parallel}$ appears slightly closer to experiment above T_N, likely reflecting the underestimation of MSRO by local quantization, although the choice of scaling could also affect the alignment of these values.

DISCUSSION

The use of fluctuations for thermodynamic calculations largely resolves the primary source of error in SMC, but a few issues remain. In particular, local quantization systematically undersamples

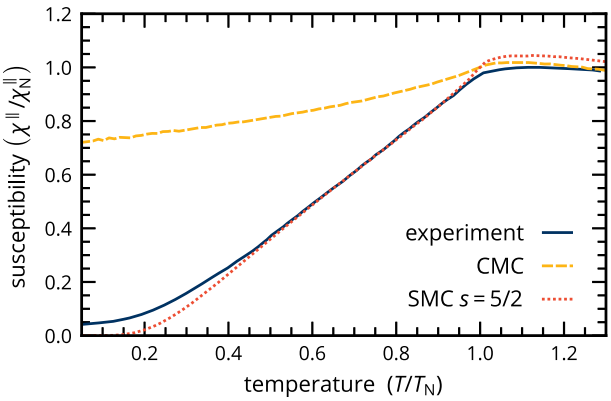

Fig. 7 Antiferromagnetic susceptibility of $RbMnF_3$. Parallel magnetic susceptibility of the Heisenberg antiferromagnet $RbMnF_3$ as a function of temperature, calculated using CMC and SMC ($s = 5/2$). Experimental data is from ref. [35]; all values are normalized relative to the Néel point to ease comparison.

low-temperature excitations, which can be seen across a range of properties in Figs. 2, 6 and 7. Magnetization, for instance, should scale as an exponential of temperature in the 0 K limit, but it appears asymptotic in Fig. 2—as shown more clearly in Supplementary Fig. 4, SMC magnetization does not significantly deviate from the ferromagnetic state below ~$T_C/5$. In reality, excitations in this region are dominated by long-wavelength spin-waves, which, while theoretically compatible with SMC, do not appear adequately sampled by local quantization. The omission of these excitations similarly explains a slight underestimation of heat capacity and susceptibility at low temperatures, as these properties reflect, respectively, energetic and magnetic fluctuations.

The absence of non-local quantizations may also be seen at higher temperatures. As shown in Fig. 6, QMC predicts slightly lower critical temperatures for $s = 1/2$ and $s = 1$ than for higher spin simulations, an effect which is not captured by SMC. For these lower quantum numbers, the locally allowed quantizations are limited and higher in energy, leaving room for lower energy, longer range excitations to play a role in the disordering transition, slightly reducing T_C from the classical values. Single-site quantization also appears to inadequately predict MSRO, as seen in Fig. 4, with the implication that quantum MSRO originates from quantization states involving multiple spins.

We hope that this work will motivate further study and development of semiclassical sampling methods, including resolutions of these issues. One apparent next step would be the simultaneous quantization of multiple neighboring spins, analogous to cluster flipping algorithms employed in CMC simulations[36]. When permuting multiple spins, new states could be drawn from the separable component of the local exact solution, which could be easily precomputed for small clusters. While extracting product states from these solutions may be nontrivial, their inclusion could allow lower energy excitations that improve simulation accuracy at low temperatures and promote high-temperature MSRO.

Opportunities for improvement notwithstanding, the simplest form of locally quantized SMC appears to provide a physics-based, parameter-free method for calculating magnetic contributions to thermodynamic properties that is at least as accurate as current methods with increased convenience and generality.

METHODS

Simulations of Fe (Figs. 2 and 5) used ten values of J_{ij} from ref. [2] for atomic separations up to and including $\mathbf{r}_{ij} = \left[\frac{3}{2}\frac{3}{2}\frac{3}{2}\right]$, which is associated with an energy several times larger than that of any longer range interaction. The selected J_{ij} predict a T_C close to the experimental value, although, given the limitations of the Heisenberg model[24], inaccuracy of the local density approximation used in parameterization[37], and neglect of temperature scaling and phonon coupling[38,39]—among other factors—the degree of accuracy presumably involves some cancellation of errors. After an equivalent period of equilibration, 10^5 MC passes were performed for $2.5 \cdot 10^5$ atoms over 1250 temperatures. For Fig. 5, similar simulations were performed at intervals of 5 K.

Simulations for Figs. 3, 4 and 6 considered 512 spins to match the QMC of ref. [3]; $5 \cdot 10^6$ MC passes were performed at 256 temperatures. Calculations of susceptibility in $RbMnF_3$ for Fig. 7 involved 10^6 passes for $1.25 \cdot 10^5$ magnetic sites.

In the case of $\mathbf{B}_k = \mathbf{0}$, the local Hamiltonian of Eq. (5) imposes no specific quantization, so trial $\mathbf{S}_k$ should be oriented randomly. While irrelevant for most simulations, this procedure ensures that $s = \frac{1}{2}$ SMC trajectories with initially collinear spins are not restricted to the original quantization axis (i.e., an Ising model), as would otherwise occur. In practice, these calculations were initialized with randomly oriented spins to avoid any such issues.

Simulations were implemented in Julia[40] and plot data from refs. [3,30,35] were reproduced using WebPlotDigitizer[41].

DATA AVAILABILITY

All the data produced in this study are available from the authors (mdasta@berkeley.edu) upon request.

CODE AVAILABILITY

All the code developed for this study is readily available from the authors (mdasta@berkeley.edu) upon request along with guidance on its implementation.

Received: 29 May 2022; Accepted: 10 August 2022;
Published online: 30 August 2022

REFERENCES

1. Halilov, S. V., Perlov, A. Y., Oppeneer, P. M. & Eschrig, H. Magnon spectrum and related finite-temperature magnetic properties: a first-principle approach. *Europhys. Lett.* **39**, 91–96 (1997).
2. Turek, I., Kudrnovský, J., Drchal, V. & Bruno, P. Exchange interactions, spin waves, and transition temperatures in itinerant magnets. *Philos. Mag.* **86**, 1713–1752 (2006).
3. Körmann, F., Dick, A., Hickel, T. & Neugebauer, J. Rescaled Monte Carlo approach for magnetic systems: ab initio thermodynamics of bcc iron. *Phys. Rev. B* **81**, 134425 (2010).
4. Körmann, F., Dick, A., Hickel, T. & Neugebauer, J. Role of spin quantization in determining the thermodynamic properties of magnetic transition metals. *Phys. Rev. B* **83**, 165114 (2011).
5. Körmann, F. et al. Free energy of bcc iron: integrated ab initio derivation of vibrational, electronic, and magnetic contributions. *Phys. Rev. B* **78**, 033102 (2008).
6. Körmann, F. et al. Temperature dependent magnon-phonon coupling in bcc Fe from theory and experiment. *Phys. Rev. Lett.* **113**, 165503 (2014).
7. Evans, R. F. L., Atxitia, U. & Chantrell, R. W. Quantitative simulation of temperature-dependent magnetization dynamics and equilibrium properties of elemental ferromagnets. *Phys. Rev. B* **91**, 144425 (2015).
8. Woo, C. H., Wen, H., Semenov, A. A., Dudarev, S. L. & Ma, P.-W. Quantum heat bath for spin-lattice dynamics. *Phys. Rev. B* **91**, 104306 (2015).
9. Bergqvist, L. & Bergman, A. Realistic finite temperature simulations of magnetic systems using quantum statistics. *Phys. Rev. Mater.* **2**, 013802 (2018).
10. Barker, J. & Bauer, G. E. W. Semiquantum thermodynamics of complex ferrimagnets. *Phys. Rev. B* **100**, 140401 (2019).
11. Sandvik, A. W. Computational studies of quantum spin systems. *AIP Conf. Proc.* **1297**, 135–338 (2010).
12. Körmann, F. *Magnetic Systems Studied by First-Principles Thermodynamics*. Ph.D. thesis (Universität Paderborn, Paderborn, Germany, 2011).
13. Takasu, S., Miyashita, S. & Suzuki, M. Thermodynamic properties of the spin-1/2 Heisenberg antiferromagnet on the triangular lattice. In *Quantum Monte Carlo Methods in Equilibrium and Nonequilibrium Systems* (Springer Series in Solid-State Sciences, Vol. 74) (ed Suzuki, M.) 114–124 (Springer, 1987).
14. Henelius, P. & Sandvik, A. W. Sign problem in Monte Carlo simulations of frustrated quantum spin systems. *Phys. Rev. B* **62**, 1102–1113 (2000).
15. Sandvik, A. W. Stochastic series expansion method for quantum Ising models with arbitrary interactions. *Phys. Rev. E* **68**, 056701 (2003).

16. Raggio, G. A. Spectral conditions on the state of a composite quantum system implying its separability. *J. Phys. A Math. Gen.* **39**, 617–636 (2006).
17. Anders, J. & Vedral, V. Macroscopic entanglement and phase transitions. *Open Syst. Inf. Dyn.* **14**, 1–16 (2007).
18. Amico, L., Fazio, R., Osterloh, A. & Vedral, V. Entanglement in many-body systems. *Rev. Mod. Phys.* **80**, 517–576 (2008).
19. Werner, R. F. Quantum states with Einstein-Podolsky-Rosen correlations admitting a hidden-variable model. *Phys. Rev. A* **40**, 4277–4281 (1989).
20. Fisher, M. E. Magnetism in one-dimensional systems—the Heisenberg model for infinite spin. *Am. J. Phys.* **32**, 343–346 (1964).
21. Månson, M. Classical limit of the Heisenberg model. *Phys. Rev. B* **12**, 400–404 (1975).
22. Ma, P.-W., Woo, C. H. & Dudarev, S. L. Large-scale simulation of the spin-lattice dynamics in ferromagnetic iron. *Phys. Rev. B* **78**, 024434 (2008).
23. Crangle, J. & Goodman, G. M. The magnetization of pure iron and nickel. *Proc. R. Soc. Lond. A. Math. Phys. Sci.* **321**, 477–491 (1971).
24. Ruban, A. V., Khmelevskyi, S., Mohn, P. & Johansson, B. Temperature-induced longitudinal spin fluctuations in Fe and Ni. *Phys. Rev. B* **75**, 054402 (2007).
25. Mook, H. A., Lynn, J. W. & Nicklow, R. M. Temperature dependence of the magnetic excitations in nickel. *Phys. Rev. Lett.* **30**, 556–559 (1973).
26. Lynn, J. W. Temperature dependence of the magnetic excitations in iron. *Phys. Rev. B* **11**, 2624–2637 (1975).
27. Capellmann, H. & Viera, V. Strong short range magnetic order in ferromagnetic transition metals above T_C: a theoretical explanation. *Solid State Commun.* **43**, 747–750 (1982).
28. Heine, V., Liechtenstein, A. I. & Mryasov, O. N. On the origin of short-range order above T_c in Fe, Co, Ni. *Europhys. Lett.* **12**, 545–550 (1990).
29. Melnikov, N. B., Reser, B. I. & Paradezhenko, G. V. Short-range order in metals above the Curie temperature. *AIP Adv.* **8**, 101402 (2018).
30. Melnikov, N., Paradezhenko, G. & Reser, B. Magnetic short-range order in Fe and Ni above the Curie temperature. *J. Magn. Magn. Mater.* **473**, 296–300 (2019).
31. Melnikov, N. B. & Reser, B. I. Magnetism of metals in the dynamic spin-fluctuation theory. *Phys. Met. Metallogr.* **117**, 1328–1383 (2016).
32. Manousiouthakis, V. I. & Deem, M. W. Strict detailed balance is unnecessary in Monte Carlo simulation. *J. Chem. Phys.* **110**, 2753–2756 (1999).
33. Wang, F. & Landau, D. P. Efficient, multiple-range random walk algorithm to calculate the density of states. *Phys. Rev. Lett.* **86**, 2050–2053 (2001).
34. Windsor, C. G. & Stevenson, R. W. H. Spin waves in $RbMnF_3$. *Proc. Phys. Soc.* **87**, 501–504 (1966).
35. Chaddha, G. & Seehra, M. Magnetization process and principal magnetic susceptibilities in $RbMnF_3$. *Solid State Commun.* **44**, 1097–1100 (1982).
36. Wang, J.-S. & Swendsen, R. H. Cluster Monte Carlo algorithms. *Phys. A Stat. Mech. Appl.* **167**, 565–579 (1990).
37. Jansen, H. J. F., Hathaway, K. B. & Freeman, A. J. Structural properties of ferromagnetic bcc iron: a failure of the local-spin-density approximation. *Phys. Rev. B* **30**, 6177–6179 (1984).
38. Yin, J., Eisenbach, M., Nicholson, D. M. & Rusanu, A. Effect of lattice vibrations on magnetic phase transition in bcc iron. *Phys. Rev. B* **86**, 214423 (2012).
39. Mankovsky, S., Polesya, S. & Ebert, H. Exchange coupling constants at finite temperature. *Phys. Rev. B* **102**, 134434 (2020).
40. Bezanson, J., Edelman, A., Karpinski, S. & Shah, V. B. Julia: a fresh approach to numerical computing. *SIAM Rev.* **59**, 65–98 (2017).
41. Rohatgi, A. WebPlotDigitizer: Version 4.5. https://automeris.io/WebPlotDigitizer (2021).

ACKNOWLEDGEMENTS

F.W. was supported by the U.S. Department of Defense through the National Defense Science and Engineering Graduate Fellowship Program. M.A. and L.-W.W. were supported by the U.S. Department of Energy, Office of Science, Office of Basic Energy Sciences, Materials Sciences and Engineering Division, under Contract No. DE-AC02-05-CH11231 (Materials Project program KC23MP and Non-Equilibrium Magnetic Materials program MSMAG, respectively). Computational resources were provided by award BES-ERCAP0021088 of the National Energy Research Scientific Computing Center (NERSC), a U.S. Department of Energy Office of Science User Facility at Lawrence Berkeley National Laboratory, operated under the same contract.

AUTHOR CONTRIBUTIONS

F.W. and L.-W.W. conceived of the approach. F.W. derived, implemented, and performed calculations in consultation with M.A. F.W. wrote the manuscript with input from M.A. and L.-W.W.

COMPETING INTERESTS

The authors declare no competing interests.

ADDITIONAL INFORMATION

Supplementary information The online version contains supplementary material available at https://doi.org/10.1038/s41524-022-00875-8.

Correspondence and requests for materials should be addressed to Mark Asta or Lin-Wang Wang.

Reprints and permission information is available at http://www.nature.com/reprints

Publisher's note Springer Nature remains neutral with regard to jurisdictional claims in published maps and institutional affiliations.